Supporting Information

Systematic probing of protein adsorption on protein-based nanoparticles in dependence of the particle surface charge

Ben Otange[#], *Tobias Katenkamp*[#], *Hendrik Böhler*, *Michael Rütten*, *Laurin Lang*, *Florian Schulz*, *Wolfgang J. Parak*[*], *Tobias Beck*[*]
[#]both authors contributed equally to this work

B. Otange, F. Schulz, W. Parak
Institute for Nanostructure and Solid State Physics
University of Hamburg
Luruper Chaussee 149, 22761 Hamburg, Germany
wolfgang.parak@uni-hamburg.de

T. Katenkamp, H. Böhler, M. Rütten, L. Lang, T. Beck
Institute of Physical Chemistry
University of Hamburg
Grindelallee 117, 20146 Hamburg, Germany
tobias.beck@uni-hamburg.de

W. J. Parak, T. Beck
Hamburg Centre for Ultrafast Imaging
University of Hamburg
Luruper Chaussee 149, Hamburg, Germany

Table of contents

Supporting materials and methods 3
Negative and Positive Ferritin Variants 3
General lab work 4
Protein Production and Purification 4
Transformation 4
Precultures 4
Production Cultures 5
Ftn^{pos}-variants 5
Ftn^{neg}-variants 5
Protein Purification 5
Ftn^{pos}-variants 5
Ftn^{neg}-variants 6
Preparation of stock solutions of fluorophores 7
Fluorophore labeling 7
Ftn^{pos}-variants 7
Ftn^{neg}-variants 8
Iron removal from Ftn^{pos}-m4-1C 8
Encapsulation of Rho6G in Ftn^{pos}-m4-1C 9
Electrostatic potential 9
Circular dichroism spectroscopy 9
Transmission electron microscopy (TEM) 10
Electrospray ionization mass spectrometry (ESI-MS) 11
Matrix-assisted laser desorption/ionization mass spectrometry (MALDI-MS) 11
UV-Vis absorption spectroscopy 12
Photoluminescence measurements 12
Zeta Potential Measurements 12
Fluorescence Correlation Spectroscopy (FCS) Measurements 13
Supporting Figures 17
Supporting Tables 25
References 34

Supporting materials and methods

Negative and Positive Ferritin Variants

Negative and positive variants of human heavy chain ferritin (Ftn) were designed and prepared to align with the mutation details provided in **Table S1**. Protein variants with a positively charged surface are: Ftn^{pos}-1C, Ftn^{pos}-m4-1C and Ftn^{pos}-A1-1C. Protein variants with a negatively charged surface are: Ftn^{neg}-1C, HF-1C and Ftn^{neg}-m8-1C. The variants Ftn^{neg}-1C and HF-1C originate from earlier work.[1] Ftn^{pos}-m4-1C, Ftn^{pos}-m8-1C and Ftn^{pos}-1C variants also come from an earlier work, but here the cysteine at position 53 was additionally introduced and all other cysteines were replaced by alanine, lysine, or glutamic acid residues.[2] The variant Ftn^{pos}-A1 was also designed previously and published by Künzle et al. as run 4.[3] In this study the cysteine mutation at position 53 was introduced.

General lab work

All chemicals were procured from commercial suppliers and were utilized without additional purification. All solutions were prepared using ultrapure water (Purelab Flex 2 system, resistivity of 18.2 MΩ·cm) and analytical grade reagents were employed whenever feasible, unless stated otherwise.

Protein Production and Purification

The process for producing $Ftn^{(neg)}$ and $Ftn^{(pos)}$ and their respective variants closely mirrors the method previously described for $Ftn^{(neg/pos)}$, with only minor modifications introduced during Ion-Exchange-Chromatography for the variants.[3]

Transformation

Calcium-competent E. coli BL21-Gold (DE3) cells (Agilent), maintained as 100 µL stocks at -80°C, were brought to an ice-cold equilibrium for 10 minutes. Simultaneously, plasmid solutions (GenScript Biotech (Netherlands) B.V.) coding for the different protein variants, stored at -20 °C, were also equilibrated on ice. Subsequently, 2 µL of a 100 ng/µL plasmid solution was gently introduced to the cells and thoroughly mixed with a pipette tip. The mixture was incubated on ice for a duration of 30 minutes. Following the ice incubation, a heat shock was induced by immersing the mixture in a water bath set at 42 °C for 45 seconds, after which it was promptly returned to ice for a 2-minute recovery period. The cells were then introduced to 0.9 mL of lysogeny broth (LB) media and incubated at 37 °C with agitation at 250 rpm for 1 hour. Following the incubation period, the cells were subjected to centrifugation at 2000 g, and 0.9 mL of the supernatant was removed. The pellet containing the cells was resuspended in the remaining solution (around 100 µL) and subsequently streaked onto LB-agar plates supplemented with 150 µg/mL ampicillin, using glass beads for uniform distribution. These streaked agar plates were left to incubate at 37 °C overnight. Plates bearing fully developed colonies were preserved at 4 °C.

Precultures

Precultures were initiated by selecting single colonies from pre-existing LB-agar plates stored at 4 °C and containing transformed E. coli BL21-Gold (DE3) cells with plasmids inside. These selected colonies were then incubated overnight in 5 mL of sterile LB-Miller medium, which was further enriched with 150 µg/mL ampicillin. Incubation was maintained at 37 °C with continuous agitation at a rate of 180 rpm.

Production Cultures

Ftn^{pos}-variants

For the primary production culture, 400 mL of LB medium was prewarmed to 37 °C and supplemented with 150 µg/mL ampicillin within 1000 mL conical glass cell culture flasks. Cells from the precultures were then introduced at a concentration of 1% (v/v). The cells were cultivated at 37 °C with continuous agitation at 200 rpm until reaching an optical density at 600 nm (OD_{600}) of 0.2. Protein overexpression was initiated by adding isopropyl β-D-1-thiogalactopyranoside (IPTG) to attain a final concentration of 0.25 mM, and the cells were further incubated for an additional 5 hours at 37 °C. Subsequently, the cells were harvested through centrifugation at 4000 g, and the resulting pellets were preserved at -20 °C for subsequent purification processes.

Ftn^{neg}-variants

For the primary production culture, 400 mL of TB medium was prewarmed to 37 °C and supplemented with 150 µg/mL ampicillin within 1000 mL conical glass cell culture flasks. Cells from the precultures were then introduced at a concentration of 1% (v/v). The cells were cultivated at 37 °C with continuous agitation at 200 rpm until reaching an OD_{600} of 0.6-0.7. Protein overexpression was initiated by adding IPTG to attain a final concentration of 0.25 mM, and the cells were further incubated for at least 48 hours at 18 °C. Subsequently, the cells were harvested through centrifugation at 4000 g, and the resulting pellets were preserved at -20 °C for subsequent purification processes.

Protein Purification

Ftn^{pos}-variants

Cells from 800 mL culture were resuspended in 20 mL 50 mM tris(hydoxymethyl)aminomethane (Tris) buffer (pH 7.5, 1 M NaCl). Cell lysis was executed in an ice bath using sonication at 60% amplitude for eight cycles, with each cycle comprising 1 minute of sonication followed by 1 minute off. An ultrasonic processor, Vibra-Cell VCX-130 (Sonics), was employed for this purpose. The resultant lysate underwent centrifugation at 14,000 g for 20 minutes to separate cell debris from soluble proteins. Denaturation of the majority of E. coli proteins was accomplished by heating the supernatant to 65 °C for 10 minutes in a water bath. Subsequently, the suspension was centrifuged at 14,000 g for 20 minutes, and the resulting pellet was discarded. The heat-shock supernatant was then subjected to incubation with 1.5 mg/mL RNAse A (Applichem) for a minimum of 3 hours at 37 °C, aiming to remove large RNA fragments bound to the positively charged protein cages. The

proteins remaining in the clarified solution were precipitated with ammonium sulfate, reaching a final concentration of 70% of its saturation concentration. After this step, centrifugation at 14,000 g for 20 minutes was carried out, and the supernatant was discarded, leaving behind the pellet. The resulting pellet was subsequently rebuffered in 10 mL 50 mM Tris buffer (pH 7.5, 1 M NaCl). The ammonium sulfate precipitation step was repeated once more, and the supernatant was discarded again, while the resulting pellet was dissolved in 50 mL of ion-exchange chromatography (IEC) loading buffer (50 mM 2-(N-morpholino)ethanesulfonic acid (MES), pH 6, 0.15 M NaCl). The sample was filtered through a 0.22 µm mixed cellulose esters syringe filter and subjected to purification through IEC with a linear gradient ranging from 50 mM MES, pH 6, 0.15 to 1.5 M NaCl. A 5 mL HiTrap™ SP HP cation exchange column (Cytiva) was employed for this process. Variants were eluted at different points during the gradient based on their overall charge. Additional dilution with salt-free buffer (50 mM MES, pH 6, 0 M NaCl) may have been necessary if excessive ammonium sulfate was carried over from previous steps to prevent sample loss during column loading. All fractions containing Ftn^{pos} were collected and subsequently concentrated to a final volume of 2 mL using an Amicon® Ultra - 15 filter unit (Merck) with a molecular weight cutoff of 30,000 Da. Finally, the sample underwent purification through gel filtration size exclusion chromatography (SEC) utilizing a HiLoad 16/600 Superdex™ 200 pg column with a running buffer consisting of 50 mM Tris (pH 7.5, 1 M NaCl). All chromatography steps were performed using an Äkta pure system from Cytiva. Fractions containing Ftn^{pos} were collected and stored at 4°C until further utilization.

Ftn^{neg}-variants

Cells from 400 mL culture were resuspended in 20 mL 50 mM Tris buffer (pH 7.5, 0.3 M NaCl). Cell lysis was executed in an ice bath using sonication at 60% amplitude for eight cycles, with each cycle comprising 1 minute of sonication followed by 1 minute off. An ultrasonic processor, Vibra-Cell VCX-130 (Sonics), was employed for this purpose. The resultant lysate underwent centrifugation at 14,000 g for 20 minutes to separate cell debris from soluble proteins. Denaturation of the majority of E. coli proteins was accomplished by heating the supernatant to 65 °C for 10 minutes in a water bath. Subsequently, the suspension was clarified by centrifugation at 14,000 g for 20 minutes, and the resulting pellet was discarded. The proteins remaining in the clarified solution were precipitated with ammonium sulfate, reaching a final concentration of 70% of its saturation concentration. After this step, centrifugation at 14,000 g for 20 minutes was carried out, and the supernatant was discarded, leaving behind the pellet. The resulting pellet was subsequently rebuffered in 10 mL 50 mM Tris buffer (pH 7.5, 0.3 M

NaCl). The ammonium sulfate precipitation step was repeated once more, and the supernatant was discarded again, while the resulting pellet was dissolved in 50 mL of IEC loading buffer (50 mM Tris, pH 7.5, 0 M NaCl). The sample was subjected to purification through IEC with a linear gradient ranging from 50 mM Tris, pH 7.5, 0 to 1 M NaCl. A 5 mL HiTrap™ Q HP anion exchange column (Cytiva) was employed for this process. Variants were eluted at different points during the gradient based on their overall charge. All fractions containing Ftn^{neg} were collected and subsequently concentrated to a final volume of 2 mL using an Amicon® Ultra - 15 filter unit (Merck) with a molecular weight cutoff of 30,000 Da. Finally, the sample underwent purification through gel filtration SEC utilizing a HiLoad 16/600 Superdex™ 200 pg column with a running buffer consisting of 50 mM Tris (pH 7.5, 0.3 M NaCl). All chromatography steps were performed using an Äkta pure system from Cytiva. Fractions containing Ftn^{neg} were collected and stored at 4 °C until further utilization.

Preparation of stock solutions of fluorophores

1 mg of maleimide functionalized Alexa Fluor 488 (AF488, Thermo Fisher), Rhodamin3B (Rho3B, ATTO-TEC) or Rhodamin6G (Rho6G, ATTO-TEC) was diluted in 200 µL water free dimethyl sulfoxide (DMSO, 99.7%; Acros Organics) to prepare a 5 mg/mL stock solution. This was stored at -20 °C for further use.

Fluorophore labeling

Ftn^{pos}-variants

One milligram of the Ftn^{pos}-variant (Ftn^{pos}-1C, Ftn^{pos}-m4-1C or FtnA1-1C), diluted in a 50 mM Tris buffer (pH 7.5, 1 M NaCl), was introduced into a 2 mL centrifugal tube containing 1.5 mL 10 mM phosphate buffer (pH 2.0, 20 mM NaCl). This mixture was incubated for 4 hours at room temperature. During this incubation period, the protein container underwent disassembly into its constituent subunits. In a 50 mL Falcon tube, 30 mL of 50 mM Tris buffer (pH 7.6, 50 mM NaCl) and 6 mL of 5 M NaCl were combined. After 4 hours, the disassembled protein solution was merged into the 50 mL Falcon tube. Following this, 14.02 µL of Rho6G, 14.28 µL of Rho3B, or 13.47 µL of AF488 from a 5 mg/mL stock solution were added, and the Falcon tube was gently inverted several times to ensure even distribution of the dye. The solution was subsequently incubated in darkness at room temperature overnight. The reassembled protein containers were concentrated utilizing an Amicon® Ultra - 15 filter unit (Merck) with a molecular weight cutoff of 30,000 Da and washed once with 15 mL of SEC buffer (50 mM Tris, pH 7.5, 1 M NaCl). Finally, the sample underwent purification through gel filtration SEC with

a HiLoad 16/600 Superdex™ 200 pg column utilizing a running buffer composed of 50 mM Tris buffer (pH 7.5, 1 M NaCl). Fractions containing Ftn^{pos}-variants were collected and preserved at 4 °C in the dark until further application.

Ftn^{neg}-variants

One milligram of the Ftn^{neg}-variant (Ftn^{neg}-1C, Ftn^{pos}-m8-1C or Ftn^{neg}-m4-1C), diluted in a 50 mM Tris buffer (pH 7.5, 0.3 M NaCl), was introduced into a 2 mL centrifugal tube containing 1.5 mL 10 mM phosphate buffer (pH 2.0, 20 mM NaCl). This mixture was incubated for 4 hours at room temperature. During this incubation period, the protein container underwent disassembly into its constituent subunits. In a 15 mL Falcon tube, 2.5 mL of 50 mM Tris buffer (pH 7.6, 50 mM NaCl) and 450 µL of 5 M NaCl were combined. After 4 hours, the disassembled protein solution was merged into the 15 mL Falcon tube. Following this, 14.19 µL Rho6G, 14.46 µL Rho3B or 13.64 µL AF488 from a 5 mg/mL stock solution were added, and the Falcon tube was gently inverted several times to ensure even distribution of the dye. The solution was subsequently incubated in darkness at room temperature overnight. The reassembled protein containers were concentrated utilizing an Amicon® Ultra - 15 filter unit (Merck) with a molecular weight cutoff of 30,000 Da and washed once with 15 mL of SEC buffer (50 mM Tris, pH 7.5, 0.3 M NaCl). Finally, the sample underwent purification through gel filtration SEC with a HiLoad 16/600 Superdex™ 200 pg column utilizing a running buffer composed of 50 mM Tris buffer (pH 7.5, 0.3 M NaCl). Fractions containing Ftn^{neg}-variants were collected and preserved at 4 °C in the dark until further application.

Iron removal from Ftn^{pos}-m4-1C

Due to iron complexation and deposition during the production of Ftn^{pos}-m4-1C, an additional iron removal protocol had to be performed. This is based on the protocol of Moglia et al. with minor modifications.[4] Ftn^{pos}-m4-1C in 50 mM Tris buffer (1 M NaCl, pH 7.5) was rebuffered to 50 mM Tris buffer (1 M NaCl, pH 4.5) utilizing an Amicon® Ultra 0.5 mL centrifugal filter with a molecular weight cutoff of 30,000 Da. The protein sample was diluted with 50 mM Tris buffer (1 M NaCl, pH 4.5) to reach a final volume of 500 µL, followed by centrifugation for 5 minutes at 12,000 g. The solution was then adjusted back to 500 µL. This rebuffering procedure was iterated five times. 40 µL of a 10% thioglycolic acid (TGA; Sigma-Aldrich) solution and 200 µL of a 0.3 M ethylenediaminetetraacetic acid (EDTA; PanReac Applichem) solution were added in a 1.5 mL centrifuge tube. 100 µL of Ftn^{pos}-m4-1C (c = 25.7 mg/mL) was added to the TGA and EDTA solution. The mixture was incubated for 1 h at 4 °C. It was then rebuffered five times with a 50 mM Tris buffer (1 M NaCl, pH 7.5) utilizing an Amicon® Ultra - 15 filter

unit (Merck) with a molecular weight cutoff of 30,000 Da. The sample underwent purification through gel filtration SEC with a HiLoad 16/600 Superdex™ 200 pg column utilizing a running buffer composed of 50 mM Tris buffer (pH 7.5, 1 M NaCl).

Encapsulation of Rho6G in Ftn^{pos}-m4-1C

One milligram of Ftn^{pos}-m4-1C diluted in a 50 mM Tris buffer (pH 7.5, 1 M NaCl) was introduced into a 2 mL centrifugal tube containing 1.5 mL 10 mM glycine buffer (pH 2.0, 20 mM NaCl). This mixture was incubated for 4 hours at room temperature. During this incubation period, the protein container underwent disassembly into its constituent subunits. In a 50 mL Falcon tube, 30 mL of 50 mM Tris buffer (pH 7.6, 50 mM NaCl) and 6 mL of 5 M NaCl were combined. After 4 h, 4.1 µL of a 20 mg/mL Tris(2-carboxyethyl)phosphine hydrochloride (TCEP-HCl, Carl Roth) stock solution was added to the disassembled protein containers. The mixture was incubated for 30 min. The solution was then rebuffered five times with a 10 mM glycine buffer (pH 2.0, 20 mM NaCl) in an Amicon® Ultra - 15 filter unit (Merck) with a molecular weight cutoff of 10,000 Da and concentrated to a volume of 1.5 mL. The disassembled protein solution was merged into the 50 mL Falcon tube. Following this, 14.02 µL of Rho6G, 5.71 µL of Rho3B, or 13.47 µL of AF488 from a 5 mg/mL stock solution were added, and the Falcon tube was gently inverted several times to ensure even distribution of the dye. The solution was subsequently incubated in darkness at room temperature overnight. The reassembled protein containers were concentrated utilizing an Amicon® Ultra - 15 filter unit (Merck) with a molecular weight cutoff of 30,000 Da and washed once with 15 mL of SEC buffer (50 mM Tris, pH 7.5, 1 M NaCl). Finally, the sample underwent purification through gel filtration SEC with a HiLoad 16/600 Superdex™ 200 pg column utilizing a running buffer composed of 50 mM Tris buffer (pH 7.5, 1 M NaCl). Fractions containing Ftn^{pos}-m4-1C were collected and preserved at 4°C in the dark until further application.

Electrostatic potential

The electrostatic potential of the Ftn-variants was calculated using the APBS tool implemented in PyMOL.[5]

Circular dichroism spectroscopy

Circular dichroism (CD) spectra were recorded on a *JASCO CD-Photometer J-815* in quartz cuvettes with a path length of 1 mm and a total volume of 100 µL. Data were measured from 190 nm to 260 nm in 0.2 nm intervals with a scanning speed of 100 nm/min. Protein solutions were rebuffered to ultrapure water utilizing an Amicon® Ultra 0.5 mL centrifugal filter with a

molecular weight cutoff of 30,000 Da. The protein samples were diluted with ultrapure water to reach a final volume of 500 µL, followed by centrifugation for 5 minutes at 12,000 g. In the final step, the volume was adjusted so that a concentration of 0.2 mg/mL was reached. For macromolecules such as proteins, the mean residue molar ellipticity $[\Theta]_{MRW}$ according to Equation S1 was used. [6] The mean residue molar concentration was calculated based on Equation S2. The results are shown in Figure S4.

$$[\Theta]_{MRW} = \frac{[\Theta]}{10\, c_r\, l} \qquad \text{(Eq. S1)}$$

$[\Theta]$	ellipticity in mdeg
c_r	mean residue molar concentration in mol/mL
l	cell path in cm (0.1 cm)

$$c_r = \frac{1000\, n\, c_g}{M_r} \qquad \text{(Eq. S2)}$$

n	number of peptide bonds (n = 4368)
c_g	Protein concentration in g/mL (c_g = 0.0002 g/mL)
M_r	Molecular weight of the protein container (see Table S1)

Transmission electron microscopy (TEM)

Ammonium molybdate stained protein samples were investigated by transmission electron microscopy to confirm the correct assembly of the nanocages after introduction of mutations. A 2% solution of ammonium molybdate (para)-hydrate (99.999%, Thermo Scientific) was freshly prepared by dissolving 20 mg of the chemical in 1 mL of ultrapure water. The solution was subsequently filtered through a 0.22 µm syringe filter (Millex, PVDF, 4 mm), discarding the initial droplets to ensure a clean staining solution. A 10 µL aliquot of the protein sample (1 mg/mL) was carefully pipetted onto a parafilm surface. Adjacent to this droplet, three 50 µL droplets of ultrapure water and two 50 µL droplets of the filtered ammonium molybdate solution were placed. A copper grid, 200 mesh, covered with Formvar and carbon (Ted Pella, 01810) with the carbon-coated side was placed face-down onto the protein sample droplet and allowed to incubate for 1 minute. Following this, the grid was sequentially washed by briefly touching it to each of the ultrapure water droplets, ensuring any residual sample was removed. A final wash was conducted with the ammonium molybdate solution by placing the grid onto a droplet of the stain solution for 1 minute. After this incubation, excess ammonium molybdate was removed by gently touching the edge of the grid to filter paper. The grid was then air-dried

for 30 minutes before imaging. All analyses were carried out with a JOEL JEM 1011 at 100kV. Micrographs showing representative areas of each grid containing the newly produced variants are shown in **Figure S5**.

Image analysis was conducted using the software ImageJ. The diameter of ferritin cages was determined through area measurement. Individual protein cages were analyzed manually, with a total of 150 particles measured for each ferritin variant. Every protein cage was outlined by drawing a circular region, and its diameter was subsequently calculated based on the measured area. The results are shown in **Figure S6.**

Electrospray ionization mass spectrometry (ESI-MS)

The dye-functionalized Ftn^{neg}-variants were rebuffered to ultrapure water utilizing an Amicon® Ultra 0.5 mL centrifugal filter with a molecular weight cutoff of 30,000 Da. The protein sample was diluted with ultrapure water to reach a final volume of 500 µL, followed by centrifugation for 5 minutes at 12,000 g. The solution was then adjusted back to 500 µL. This rebuffering procedure was iterated five times, resulting in a final concentration of approximately 3 mg/mL. To determine the mass of the dye-loaded proteins, electron-spray ionization time-of-flight mass spectrometry (Agilent 6224 ESI-TOF-MS) was employed. The measurements were conducted in positive mode, covering a mass range of m/z 110 to 3200 Da (m/z refers to the mass m of the ion X^{z-} as normalized to the unified atomic mass unit, divided by the charge state z of the ion), with a data acquisition rate of 1.03 spectra per second. The source temperature was maintained at 325 °C, the drying gas flow at 10 L/min, the nebulizer pressure at 15 psig, and the capillary voltage was set to 4000 V. Data interpretation was carried out using MestReNova software. The outcomes confirming the successful preparation of the dye-functionalized protein variant are presented in **Table S2**.

Matrix-assisted laser desorption/ionization mass spectrometry (MALDI-MS)

The dye-functionalized Ftn^{pos}-variants were rebuffered to ultrapure water utilizing an Amicon® Ultra 0.5 mL centrifugal filter with a molecular weight cutoff of 30,000 Da. The protein sample was diluted with ultrapure water to reach a final volume of 500 µL, followed by centrifugation for 5 minutes at 12,000 g. The solution was then adjusted back to 500 µL. This rebuffering procedure was iterated five times, resulting in a final concentration of approximately 3 mg/mL. To determine the mass of the dye-loaded proteins, matrix-assisted laser-desorption ionization

time-of-flight mass spectrometry (rapifleX Bruker, UKE) was employed. The measurements were conducted in positive mode, covering a mass range of m/z 5000 to 24000 Da. The matrix used was either 2',6'-Dihydroxyacetophenon (DHAP) or 2,5-dihydroxybenzoic acid (DHB). Data interpretation was carried out using MestReNova software. The outcomes confirming the successful preparation of the dye-functionalized protein variant are presented in **Table S2**.

UV-Vis absorption spectroscopy

The dye-functionalized Ftn-variants were diluted with the appropriate buffer (Ftn^{pos}: 50 mM Tris, 1 M NaCl, pH 7.5 and Ftn^{neg}: 50 mM Tris, 0.3 M NaCl, pH 7.5) to reach a final volume of 1000 µL and a final concentration of approximately 1 mg/mL. The samples were measured in quartz cuvettes (Hellma Analytics, 10x2 mm) using a Cary 60 UV-Vis Spectrophotometer in a spectral range from λ = 450 – 600 nm.

Photoluminescence measurements

The dye-functionalized Ftn-variants were diluted with the appropriate buffer (Ftn^{pos}: 50 mM Tris, 1 M NaCl, pH 7.5 and Ftn^{neg}: 50 mM Tris, 0.3 M NaCl, pH 7.5) to reach a final volume of 1000 µL and a final concentration of approximately 1 mg/mL. The samples were measured in quartz cuvettes (HellmaAnalytics, 10x2 mm) using a Fluoromax 4000 at an excitation wavelength of λ_{ex} = 400 nm.

Zeta Potential Measurements

To test the surface charges of the protein-caged nanoparticles, Laser Doppler Anemometry (LDA) was applied. As the surface charge could not be directly assessed experimentally, instead, the zeta potential of the protein cages was measured.

Zeta potential (ζ) measurements were carried out using a Zetasizer Pro Blue (Malvern Panalytical) equipped with He-Ne laser (λ = 632.8 nm) at a backscattering angle of 173°. All samples were equilibrated (120 s, 25 °C) prior to measurement. Reported ζ was averaged from three runs. Samples were measured in disposable folded capillary cells (DTS1070, Malvern Panalytical). They were washed with ethanol (3 x 3 mL) and water (3 x 3 mL) before used. Protein samples were concentrated utilizing an Amicon® Ultra - 15 filter unit (Merck) with a molecular weight cutoff of 30,000 Da and washed once with 500 µL of ultrapure water. After that, the samples were diluted with 1 mL of ultrapure water to reach a final concentration between 0.5 and 1 mg/mL. A drift-voltage of 150 V was applied. The zeta potentials of the samples were automatically generated from the instrument by measuring the electrophoretic light scattering using the

following parameters: temperature maintained at 25 °C, refractive index of 1.45 (protein), dispersant water with a refractive index of 1.33 and a viscosity of 0.8872 mPa·s.

Fluorescence Correlation Spectroscopy (FCS) Measurements

To evaluate the differential adsorption of BSA onto the electrostatically different potential variant cages, a Confocal Light Scanning Microscope (CLSM) (LSM 880, Zeiss, Germany) equipped with a fluorescence correlation spectroscopy module (Zeiss) was used. Prior to making FCS measurements, the set-up was calibrated to determine the confocal volume present in the FCS measurements. Rhodamine 6G dye (Rho6G, Lot. 80K1967, EC No. 213-584-9, Sigma) with a known diffusion coefficient (D_{Rho6G} = 414 ± 1 $\mu m^2 s^{-1}$) was used in calibration.[7] For both calibration and subsequent measurements, a dilute solution of the sample was prepared by dissolving the dye or the protein cages in deionized water at a nanomolar concentration. A nanomolar concentration is necessary to maximize the fluctuations of fluorophores diffusing in and out of the confocal volume during the FCS measurements.[8] 100 µl of 1 nM Rho6G solution was sandwiched between an 18 × 18 mm cover glass (Ref Code.0102032, No. 1.5, Paul Marlefeld GmbH & Co. KG, Germany) of thickness 0.17 mm ± 0.005 mm and a 35 mm diameter Petri dish with a glass bottom (Cat.No: 81158, Lot. 221223/1, ibidi GmbH, Germany). The sample was then quickly transferred to the CLSM stage. A 488 nm laser (0.2 laser power on the Zeiss FCS set-up scale) was focused on the sample using a Zeiss PlaN-Apochromat ×40/1.0 Water DIC (WD: 2.5 mm) objective integrated within the FCS set-up. After focusing the laser on the dye solution, the emitted fluctuating fluorescence intensity I(t) from the fluorophores upon laser irradiation, which were diffusing in and out the focus, was used to determine the diffusion time τ_{Rho6G}. Five averaged measurements each with 10 measurements were acquired per sample concentration. Based on the Gaussian surface ellipsoid approximation of the confocal volume, the lateral radius ω_x of the confocal volume was obtained from averaged diffusion time τ_{Rho6G} and known diffusion coefficient D_{Rho6G} of the dye using Equation S3.

$$\omega_x = (4D_{Rh6G}\tau_{Rh6g})^{\frac{1}{2}} \qquad \text{(Eq. S3)}$$

The ratio of the axial radius ω_z to the lateral radius ω_x is defined by a structural parameter S through the relation in Equation S4. The structural parameter for the Zeiss CLSM is fixed at S = 5.[9] Hence, applying the calculated value of ω_x from Eq. S3 and the value of S in Eq. S4 yields the unknown value of ω_z. The respective values as determined in this study were τ_{Rho6G}

= 23.9 ± 0.05 µs, $\omega_x = 0.199\ \mu m$, and $\omega_z = 0.995\ \mu m$. A sketch of the confocal volume is given in Figure S1A.

$$S = \frac{\omega_z}{\omega_x} \qquad \text{(Eq. S4)}$$

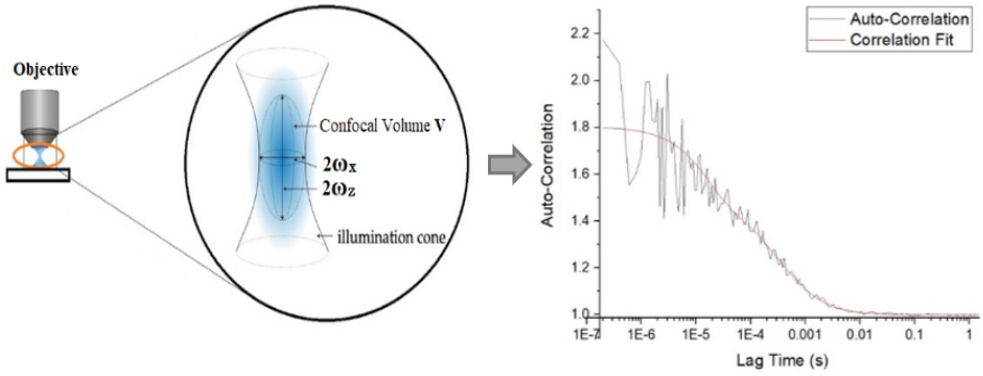

Figure S1: A) Schematic representation of the confocal volume. B) Autocorrelation (black line) and correlation fit (red line) G(τ) in dependence of the lag time τ.

From the fluctuating fluorescence intensities I(t) due to fluorophores or fluorescence-labeled protein cages diffusing in and out of the focal volume, the Zeiss ZEN software simultaneously records an autocorrelation function G(τ) from the maximum correlation (τ → 0) to a point when the correlation between the fluorescence intensity from the same fluorophore after a short time interval (τ >> 0) is 1 (i.e. no correlation). From the autocorrelation G(τ) the diffusion time τ_D of the investigated fluorophore/fluorescence-labelled protein cage was determined according to Equation S5.

$$G(\boldsymbol{\tau}) = \frac{1}{N}\left(1 + \frac{T}{1-T}e^{\frac{-t}{\tau_T}}\right)\left(\frac{1}{1+{}^{\tau}/_{\tau_D S^2}}\right)^{\frac{1}{2}} \qquad \text{(Eq. S5)}$$

N is the number of fluorophores/fluorescent protein cages irradiated within the effective confocal volume (as defined ω_x and ω_z and according to Eq. S4), $\boldsymbol{\tau}_D$ is the time of diffusion across the confocal volume, $\boldsymbol{\tau}_T$ is the triplet lifetime/triplet relaxation time and T is the fraction of the triplet state decay. In the case of Rhodamine 6G the fit parameters were $\tau_T = 0.575 \pm 0.15$ µs and T = 8.78%. The diffusion coefficient D is calculated from the radius of the confocal volume ω_x and the diffusion time $\boldsymbol{\tau}_D$ according to Eq. S6.

$$D = \frac{\omega_x^2}{4\tau_D} \quad \text{(Eq. S6)}$$

Fluorescence can apart from an excited singlet state also occur from an excited triplet state. The fluorescence emission emanating from the triplet transition (which has a longer fluorescence lifetime than the singlet emission) needs to be taken care of, as fluctuations in fluorescence intensities may be also due to triplet emission, and not only due to diffusion.[10] When the excitation is such that it causes a higher triplet state transition, the photostability of a fluorophore and its fluorescence intensity are effectively reduced to the extent that the fluctuations due to diffusion are highly compromised.[11] However, with a triplet lifetime shorter (typically less than 10 μs) than the time of diffusion τ_D, the contribution of the transition aspect of fluorescence intensity fluctuation is effectively reduced.[9] To solve this challenge, we illuminated the samples with low laser power (0.2% setting in the Zeiss CLSM) to lower the occupation of the triplet state and further triplet transition.

It is important to note that although it is recommended that the number of particles passing through the effective confocal volume should be as low as possible, the photostability of dye and nanoparticle conjugates was much lower at a corresponding lower concentration. Following the recommendation of a few particles within the confocal volume would warrant the need for higher laser power, which would however simultaneously increase the measurement problem linked to triplet state occupation. The desired number of particles was obtained through the application of Equation S7 connecting the molar fluorophore/protein cage concentration c to the number N of fluorophores/protein cages in the confocal volume V.

$$c = \frac{N}{N_A V} \quad \text{(Eq. S7)}$$

$N_A = 6.023 \cdot 10^{23}$ is Avogadro's number.

Prior to incubation of the nanoparticles (i.e. protein cages) with different concentrations of bovine serum albumin (BSA, Cas Number 9048-46-8 Sigma Aldrich), we diluted the nanoparticle concentration to yield about 16 particles within the confocal volume so that further dilution through incubation would reduce the number of particles to about 8. Then 50 μL of the diluted nanoparticles (protein cages) were mixed in a ratio of 1:1 (dilution factor of 2) with solutions of different BSA concentrations diluted in deionized water, followed by incubation in darkness for 10 minutes. The samples were then loaded on the CLSM stage to determine their corresponding diffusion coefficient D after applying the autocorrelation fitting relation in

Equation S5. From the diffusion coefficient measurements obtained from each sample, the corresponding hydrodynamic radii r_h were calculated using Stokes-Einstein's relation (Equation S8).[7]

$$r_h = \frac{k_B T}{6\pi\eta D} \qquad \text{(Eq. S8)}$$

Here k_B = 1.38·10^{-23} JK^{-1}, T = 298.15 K, and η = 8.9·10^{-4} Pa.s. The viscosity η in Stokes-Einstein's relation is only applicable for low protein concentration (c_{BSA} < 100 μM), where the particle motion resistance within the solution is primarily contributed by the buffer. However, with higher protein concentrations the contribution of the excess protein particles within the buffer affects the motion of the diffusing particles, thus warranting the need for viscosity correction. A linear dependence of sample viscosity on the concentration of protein is given by Equation S9.[8]

$$\eta = (\eta_i \cdot C_{BSA} + 1)\eta_0 \qquad \text{(Eq. S9)}$$

Here η_i is the intrinsic viscosity of the BSA (3.7·10^{-3} m^{3}kg^{-1}).[12] C_{BSA} is the mass concentration of BSA, and η_0 is the viscosity of the pure buffer (here water; η_0 = 8.9·10^{-4} Pas^{-1} at 25 °C). Note that for very high protein concentrations the assumption of Eq. S9 fails.[13] It was noted that the hydrodynamic radius of the samples increased with the protein concentration until saturation level. Further increase in hydrodynamic radius beyond the saturation level could be linked to protein-protein interaction and not to protein adsorption on the nanoparticles.[14]

Supporting Figures

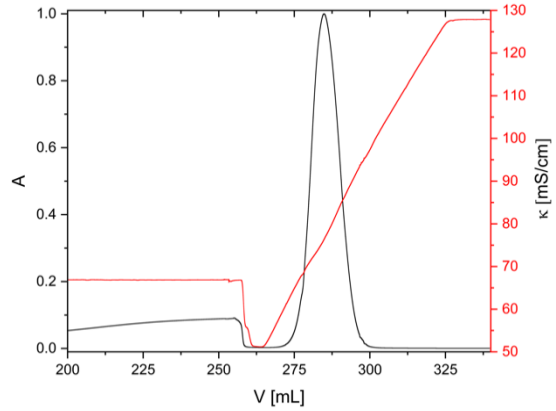

Ftn^{pos}-1C
κ = 76.3 mS/cm

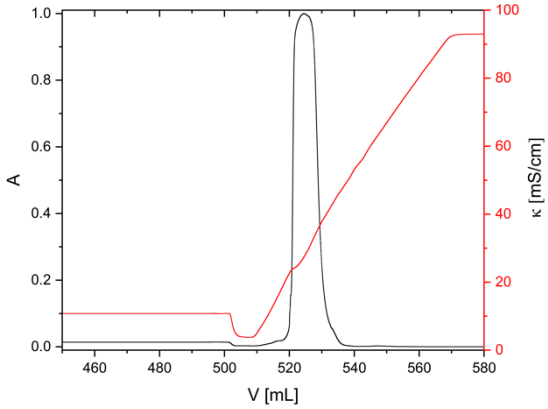

Ftn^{neg}-m8-1C
κ = 27.4 mS/cm

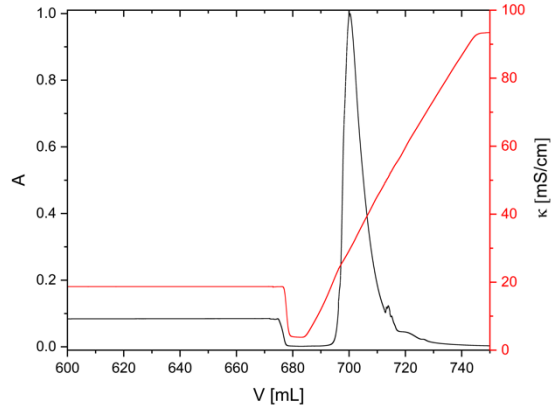

HF-1C
κ = 29.7 mS/cm

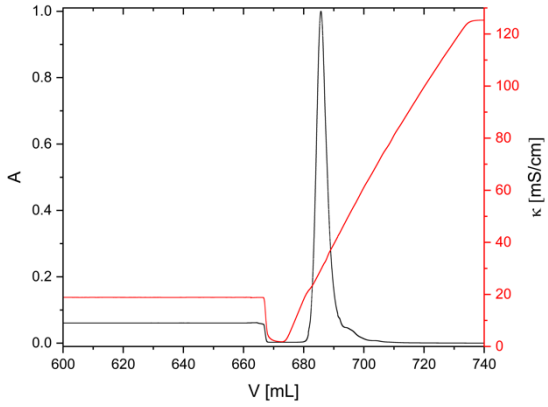

Ftn^{pos}-A1-1C
κ = 29.5 mS/cm

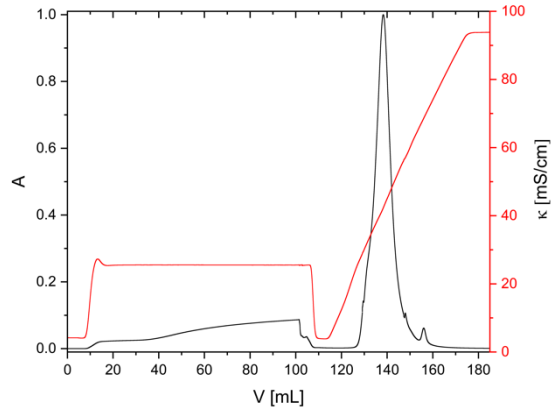

Ftn^{neg}-1C
κ = 42.2 mS/cm

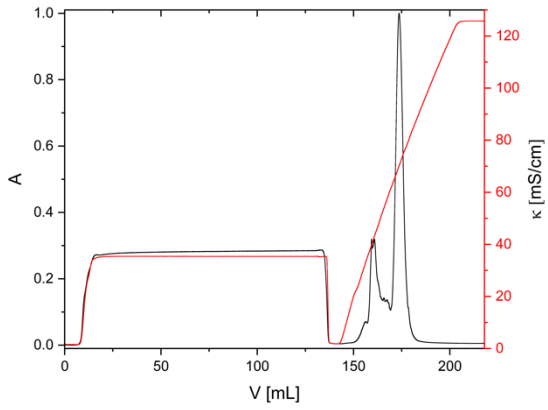

Ftn^{pos}-m4-1C
κ = 70.2 mS/cm

Figure S2: Normalized IEC of all Ftn-variants. The absorbance A at 280 nm (A_{280}) and the conductivity κ is plotted versus the eluted volume V.

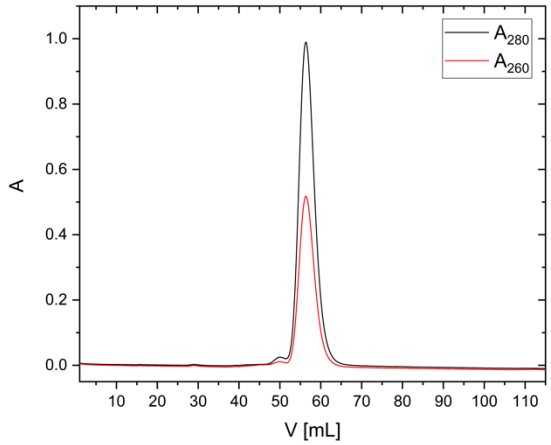

Ftn^{pos}-1C

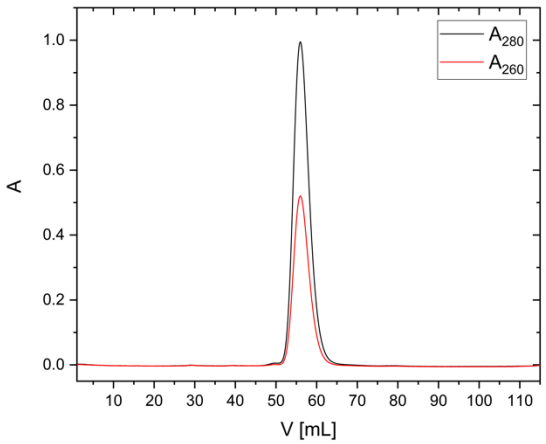

Ftn^{neg}-m8-1C

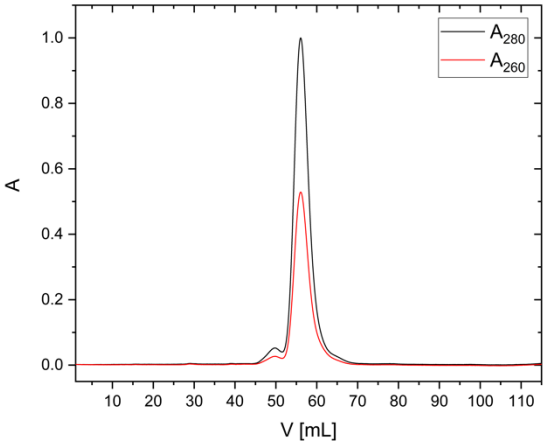

HF-1C

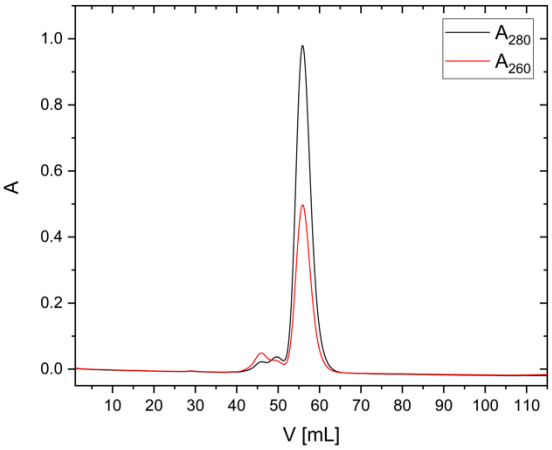

Ftn^{pos}-A1-1C

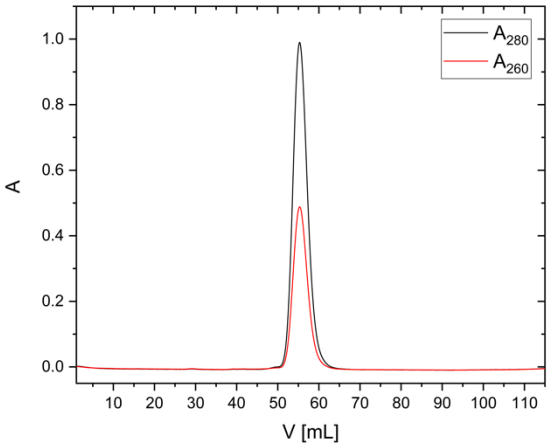

Ftn^{neg}-1C

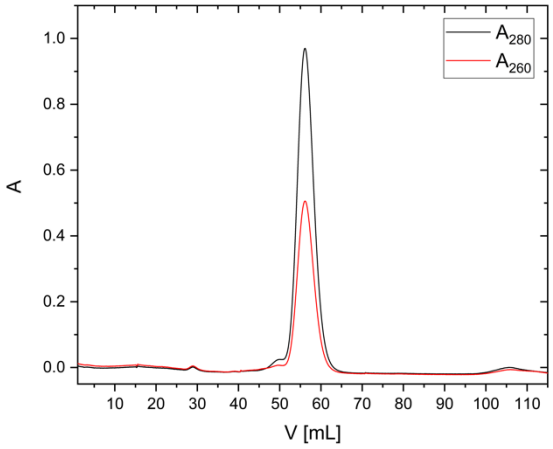

Ftn^{pos}-m4-1C – after iron removal

Figure S3: Normalized second SEC of all Ftn-variants. The absorbance A at 260 nm (A_{260}) and 280 nm (A_{280}) is plotted versus the eluted volume V.

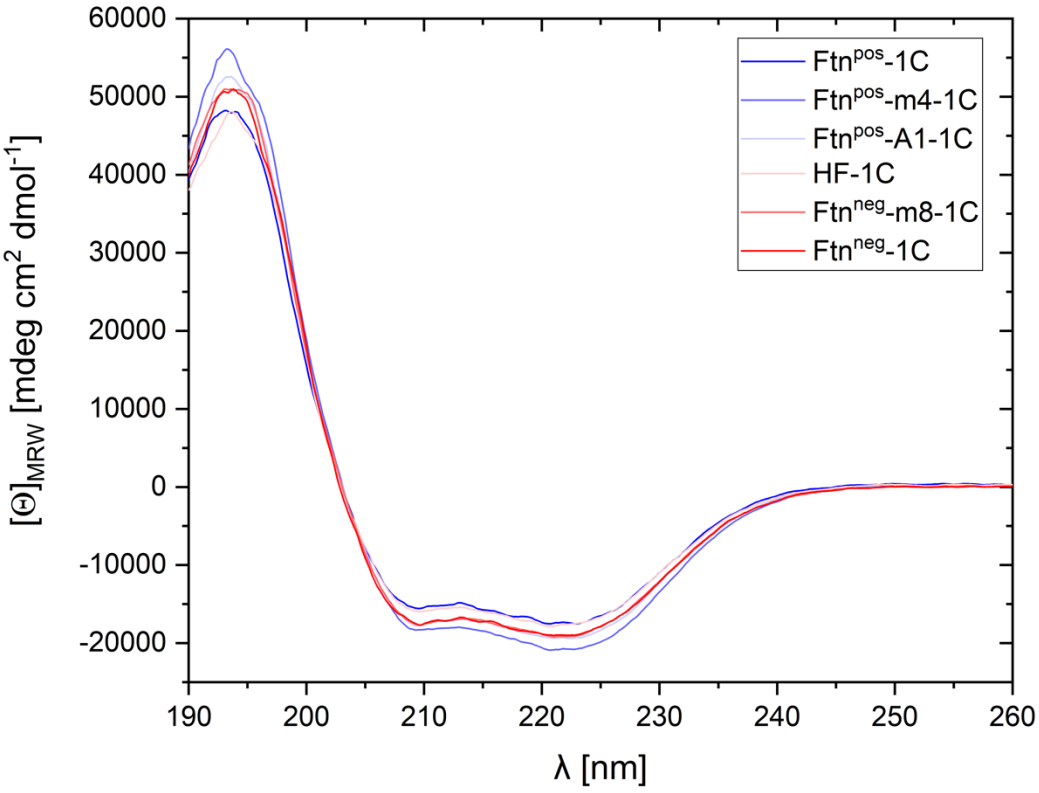

Figure S4: CD spectra of all ferritin variants. The mean residue molar ellipticity $[\Theta]_{MRW}$ is plotted versus the wavelength λ from 190 nm to 260 nm.

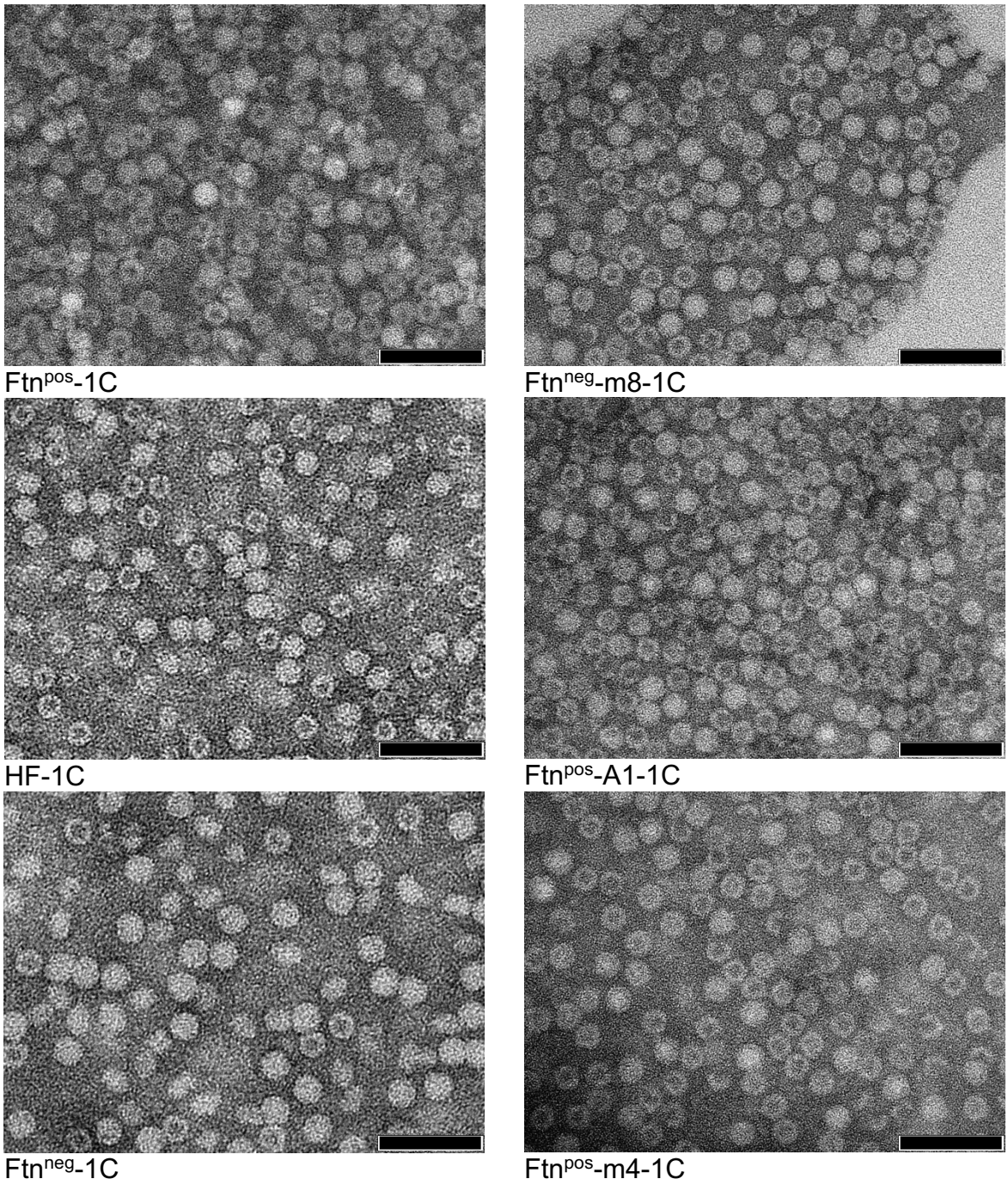

Figure S5: Negative stained TEM images of all Ftn-variants. A 2% ammonium molybdate solution was used for negative staining. The scale bar is 50 nm.

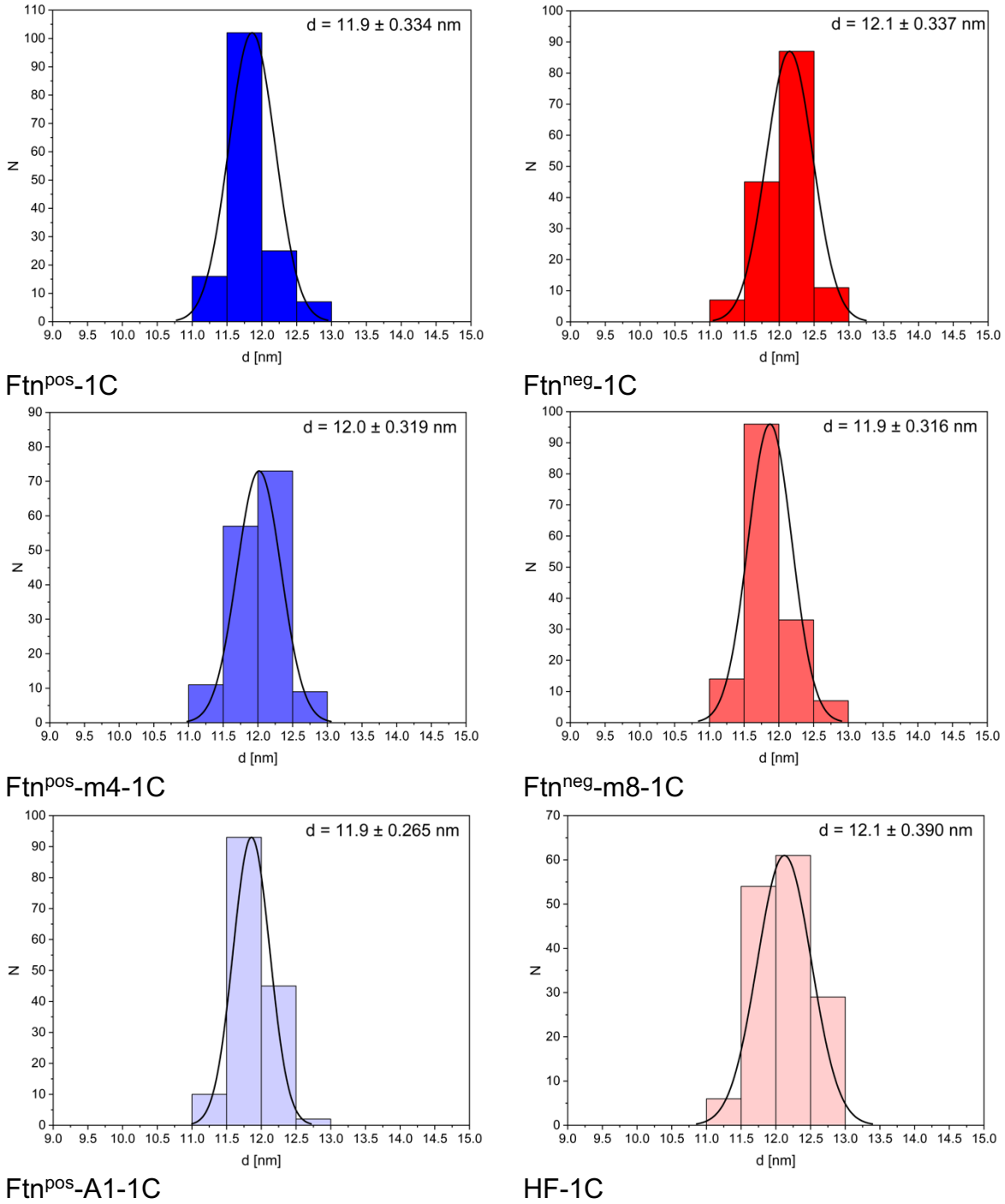

Figure S6: Size distribution of all Ftn variants as determined by negative stained TEM images, showing the number of counts *N* with which protein cages with diameter *d* were found. For each ferritin variant, 150 protein cages were counted.

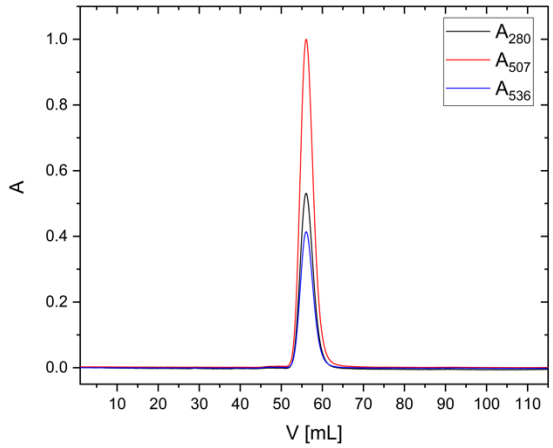

Ftn^{pos}-1C-Rho6G
A_{507}/A_{280} = 1.81
A_{536}/A_{280} = 0.83

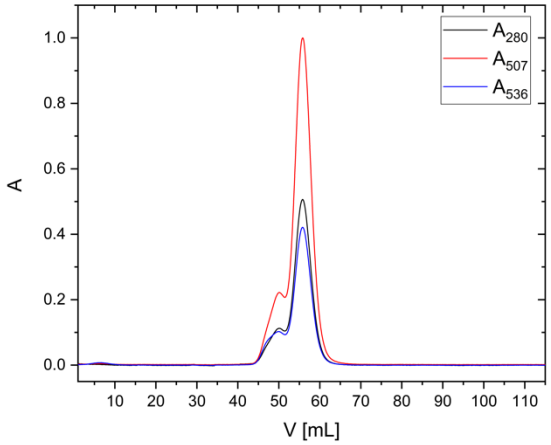

Ftn^{neg}-m8-1C-Rho6G
A_{507}/A_{280} = 1.97
A_{536}/A_{280} = 0.83

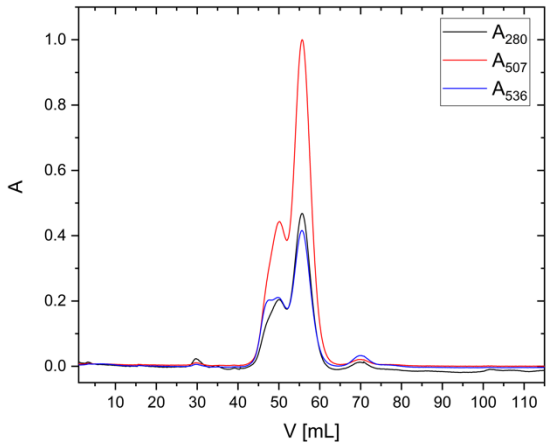

HF-1C-Rho6G
A_{507}/A_{280} = 1.90
A_{536}/A_{280} = 0.92

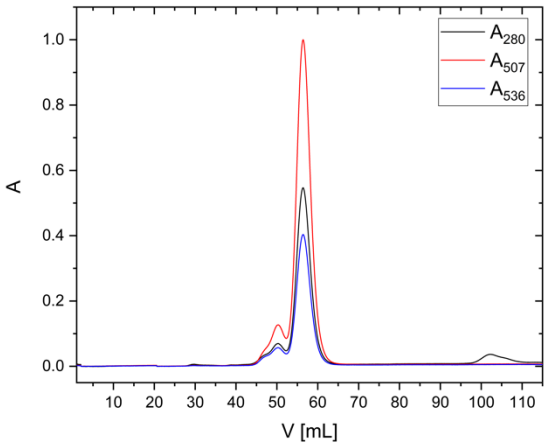

Ftn^{pos}-A1-1C-Rho6G
A_{507}/A_{280} = 1.83
A_{536}/A_{280} = 0.74

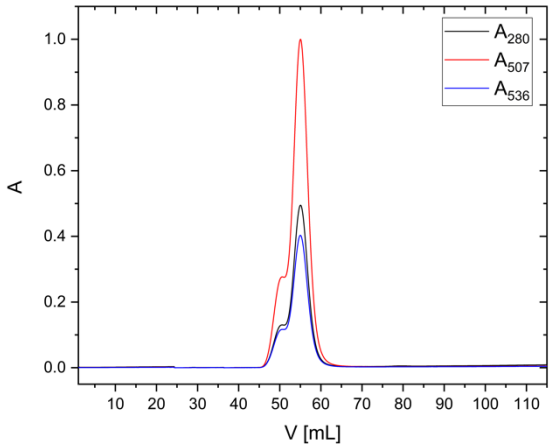

Ftn^{neg}-1C-Rho6G
A_{507}/A_{280} = 2.02
A_{536}/A_{280} = 0.81

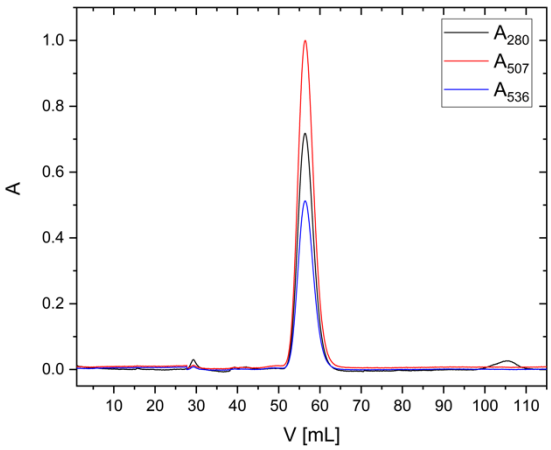

Ftn^{pos}-m4-1C-Rho6G
A_{507}/A_{280} = 1.39
A_{536}/A_{280} = 0.71

Figure S7: Normalized SEC after encapsulation of Rho6G in all Ftn-variants. The absorbance A at 280 nm (A_{280}), 507 nm (A_{507}) and 536 nm (A_{536}) is plotted versus the eluted volume V.

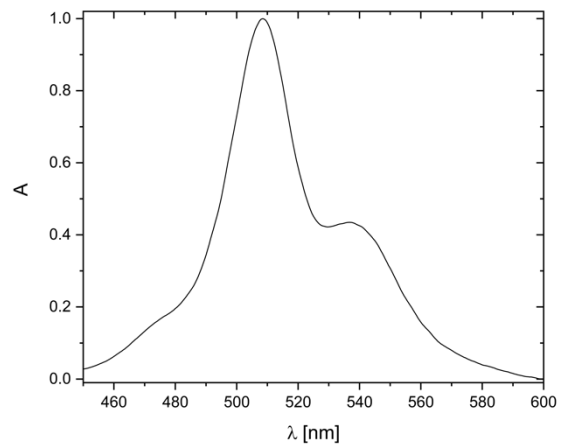

Ftn^{pos}-1C-Rho6G

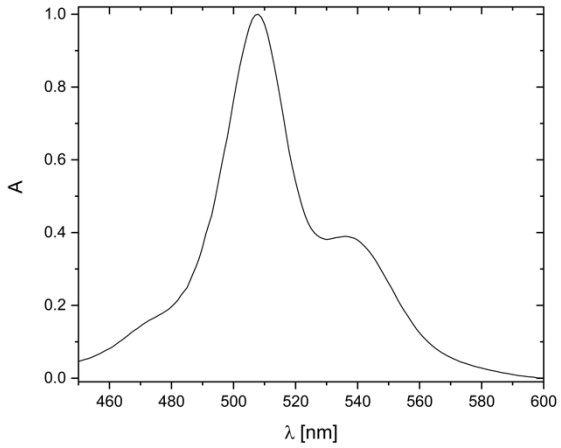

Ftn^{neg}-m8-1C-Rho6G

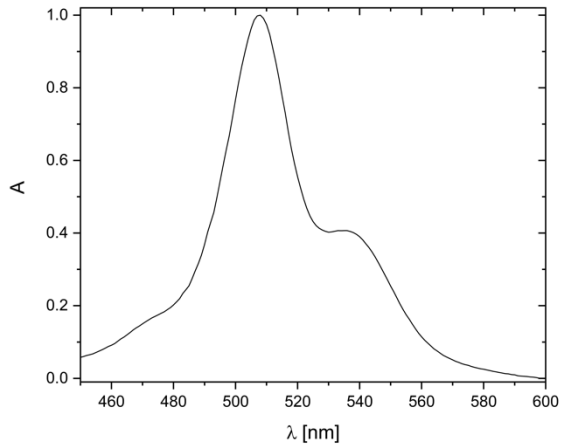

HF-1C-Rho6G

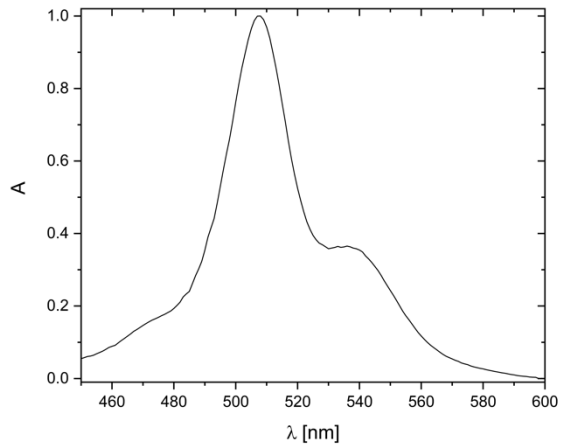

Ftn^{pos}-A1-1C-Rho6G

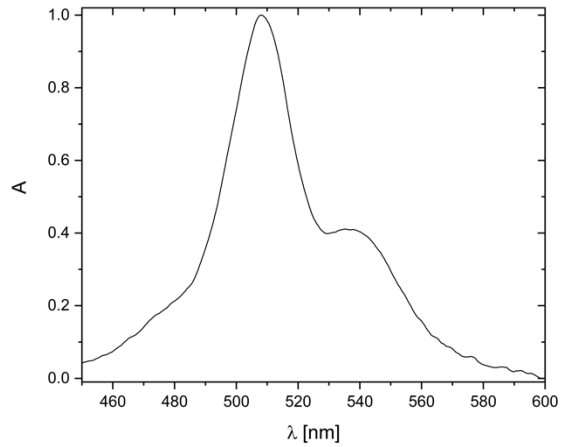

Ftn^{neg}-1C-Rho6G

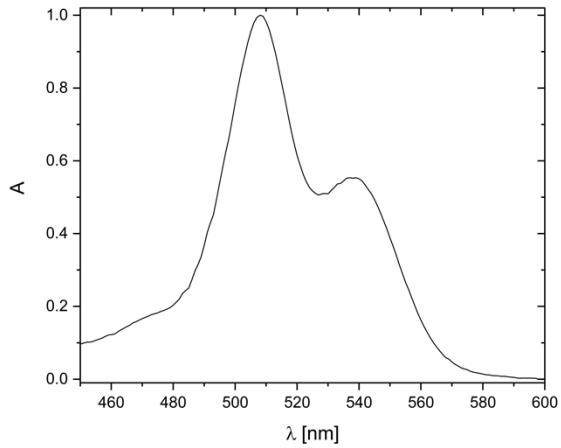

Ftn^{pos}-m4-1C-Rho6G

Figure S8: Normalized UV-Vis absorption spectra of all Ftn-variants with Rho6G. The absorption A is plotted versus the wavelength λ.

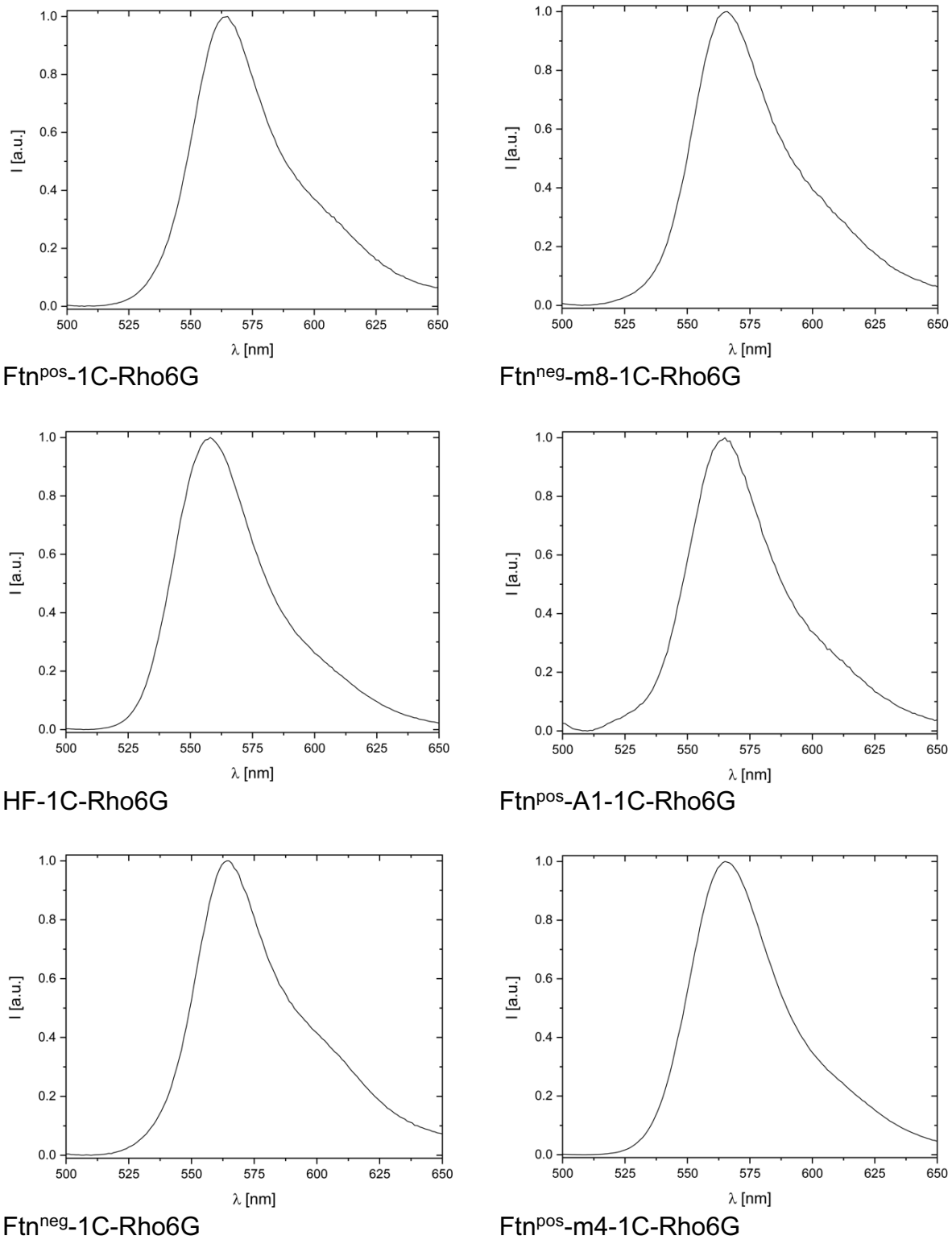

Figure S9: Normalized photoluminescence spectra of all Ftn-variants with Rho6G. The emission intensity I (under excitation at λ_{ex} = 400 nm) is plotted versus the wavelength λ.

Supporting Tables

Table S1: Mutations present on negatively and positively charged ferritin variants. All variants are shown with their respective mutations starting from native human heavy chain ferritin. Mutations are indicated by the one letter code for the native residue followed by the position in the protein chain followed by the new residue that has been introduced. The molecular weight M_W, number of residues, as well as DNA sequence and protein sequence are shown for each variant.

Variant Name	M_W [g mol^{-1}]	residues	Description
HF-1C	20973.23	182	Mutations: C90A, C102A, C130A, K53C DNA sequence: ACA ACC GCA TCT ACG TCA CAA GTT CGT CAG AAC TAT CAC CAA GAT AGT GAA GCT GCC ATT AAT CGC CAG ATT AAC CTG GAA CTG TAT GCC TCC TAT GTG TAT CTG AGC ATG AGC TAC TAC TTT GAT CGC GAT GAC GTT GCG CTC AAG AAC TTT GCC TGC TAC TTC TTG CAT CAG AGC CAT GAA GAA CGT GAA CAC GCG GAA AAA CTC ATG AAA CTG CAG AAT CAA CGT GGA GGT CGG ATT TTT CTG CAG GAC ATC AAG AAA CCG GAT GCG GAT GAT TGG GAA TCT GGG CTT AAC GCG ATG GAA GCA GCT CTG CAT CTG GAG AAA AAC GTG AAT CAG TCG TTA CTG GAG TTA CAC AAA CTT GCG ACT GAC AAG AAC

			GAT CCG CAT TTG GCG GAC TTC ATC GAA ACC CAT TAC CTG AAT GAA CAG GTA AAA GCC ATC AAA GAG CTG GGC GAT CAT GTC ACC AAT CTG CGC AAA ATG GGT GCT CCA GAA TCG GGC TTG GCA GAG TAT CTG TTC GAC AAA CAC ACG TTA GGC GAT AGT GAC AAC GAG TCC Protein sequence: TTASTSQVRQNYHQDSEAAINRQINLELY ASYVYLSMSYYFDRDDVALKNFACYFLH QSHEEREHAEKLMKLQNQRGGRIFLQDIK KPDADDWESGLNAMEAALHLEKNVNQS LLELHKLATDKNDPHLADFIETHYLNEQV KAIKELGDHVTNLRKMGAPESGLAEYLF DKHTLGDSDNES
Ftn^{neg}-1C	21139.27	182	Mutations: A18E, K86Q, C90E, C102E, H105E, C130A, K53C DNA sequence: ACC ACA GCA TCA ACG AGC CAA GTT CGC CAA AAC TAT CAC CAG GAT TCT GAG GAA GCG ATT AAT CGG CAG ATT AAC CTG GAG TTA TAT GCG AGC TAT GTG TAT CTG TCG ATG AGC TAC TAC TTT GAC CGT GAC GAT GTT GCA CTG AAG AAC TTT GCG TGT TAC TTT CTG CAT CAG TCC CAT GAA GAA CGC GAA CA TGC CGA GAA ACT

			GAT GAA ACT GCA GAA TCA ACG TGG TGG ACG CAT TTT CTT GCA AGA TAT CCA GAA ACC GGA TGA AGA TGA CTG GGA AAG TGG CTT GAA TGC CATG GAA GAA GCA CTG GAA CTT GAG AAG AAC GTG AAT CAG TCT CTG CTT GAA CTG CAT AAA CTG GCC ACT GAC AAG AAC GAT CCG CAT CTG GCC GAT TTC ATC GAA ACC CAC TAT CTG AAC GAA CAG GTC AAA GCG ATC AAA GAA CTC GGG GAT CAC GTA ACC AAC CTC CGT AAA ATG GGT GCT CCA GAG AGT GGC TTG GCT GAA TAC TTA TTC GAC AAA CAC ACG TTA GGC GAT TCG GAC AAT GAG TCC Protein sequence: TTASTSQVRQNYHQDSEEAINRQINLELY ASYVYLSMSYYFDRDDVALKNFACYFLH QSHEEREHAEKLMKLQNQRGGRIFLQDIQ KPDEDDWESGLNAMEEALELEKNVNQSL LELHKLATDKNDPHLADFIETHYLNEQVK AIKELGDHVTNLRKMGAPESGLAEYLFD KHTLGDSDNES
Ftn^{pos}-1C	21273.90	182	Mutations: K86Q, A18K, C90K, N98R, C102K, H105K, C130A, N25R, N109K, D123K, E162R, K53C DNA sequence: ACC ACA GCT AGT ACG TCC CAA GTA CGT CAG AAC TAT CAC CAA GAT AGC GAG AAA GCC ATT AAT

			CGC CAA ATT CGC TTG GAA CTG TAT GCA TCG TAT GTC TAC CTG TCA ATG AGC TAC TAC TTT GAT CGT GAT GAT GTT GCT CTG AAG AAC TTT GCG TGC TAC TTT CTG CAT CAG TCT CAT GAA GAA CGC GAA CAT GCC GAG AAA CTG ATG AAA CTG CAG AAT CAG CGT GGT GGA CGC ATC TTC TTA CAG GAC ATT CAG AAA CCG GAT AAA GAC GAT TGG GAA AGC GGG TTG CGT GCG ATG GAG AAA GCA CTG AAA CTG GAA AAG AAA GTG AAT CAG TCT CTG CTG GAA CTC CAC AAA TTA GCG ACG AAG AAG AAC GAT CCG CAT CTC GCC GAC TTC ATC GAA ACC CAC TAT TTA AAC GAG CAA GTG AAA GCG ATC AAA GAA CTT GGC GAT CAC GTT ACC AAC CTT CGG AAA ATG GGT GCA CCA CGC AGT GGC TTG GCC GAA TAT CTG TTC GAC AAA CAT ACT CTG GGC GAT TCC GAC AAT GAG TCG Protein sequence: TTASTSQVRQNYHQDSEKAINRQIRLELY ASYVYLSMSYYFDRDDVALKNFACYFLH QSHEEREHAEKLMKLQNQRGGRIFLQDIQ KPDKDDWESGLRAMEKALKLEKKVNQS LLELHKLATKKNDPHLADFIETHYLNEQV KAIKELGDHVTNLRKMGAPRSGLAEYLF DKHTLGDSDNES

Ftn^{pos}-m4-1C	21169.62	182	Mutations: K86Q, A18K, C90K, C102A, N25R, D123K, C130A, E162R, K53C DNA sequence: ACC ACA GCT AGT ACG TCC CAA GTA CGT CAG AAC TAT CAC CAA GAT AGC GAG AAA GCC ATT AAT CGC CAA ATT CGC TTG GAA CTG TAT GCA TCG TAT GTC TAC CTG TCA ATG AGC TAC TAC TTT GAT CGT GAT GAT GTT GCT CTG AAG AAC TTT GCG TGC TAC TTT CTG CAT CAG TCT CAT GAA GAA CGC GAA CAT GCC GAG AAA CTG ATG AAA CTG CAG AAT CAG CGT GGT GGA CGC ATC TTC TTA CAG GAC ATT CAG AAA CCG GAT AAA GAC GAT TGG GAA AGC GGG TTG AAT GCG ATG GAG GCA GCA CTG CAC CTG GAA AAG AAC GTG AAT CAG TCT CTG CTG GAA CTC CAC AAA TTA GCG ACG AAG AAG AAC GAT CCG CAT CTC GCC GAC TTC ATC GAA ACC CAC TAT TTA AAC GAG CAA GTG AAA GCG ATC AAA GAA CTT GGC GAT CAC GTT ACC AAC CTT CGG AAA ATG GGT GCA CCA CGC AGT GGC TTG GCC GAA TAT CTG TTC GAC AAA CAT ACT CTG GGC GAT TCC GAC AAT GAG TCG Protein sequence: TTASTSQVRQNYHQDSEKAINRQIRLELY ASYVYLSMSYYFDRDDVALKNFACYFLH QSHEEREHAEKLMKLQNQRGGRIFLQDIQ KPDKDDWESGLNAMEAALHLEKNVNQS

			LLELHKLATKKNDPHLADFIETHYLNEQV KAIKELGDHVTNLRKMGAPRSGLAEYLF DKHTLGDSDNES
Ftn^{neg}-m8-1C	21030.28	182	Mutations: K86Q, A18K, C90A, C102A, C130A, K53C DNA sequence: ACC ACA GCT AGT ACG TCC CAA GTA CGT CAG AAC TAT CAC CAA GAT AGC GAG AAA GCC ATT AAT CGC CAA ATT AAC TTG GAA CTG TAT GCA TCG TAT GTC TAC CTG TCA ATG AGC TAC TAC TTT GAT CGT GAT GAT GTT GCT CTG AAG AAC TTT GCG TGC TAC TTT CTG CAT CAG TCT CAT GAA GAA CGC GAA CAT GCC GAG AAA CTG ATG AAA CTG CAG AAT CAG CGT GGT GGA CGC ATC TTC TTA CAG GAC ATT CAG AAA CCG GAT GCG GAC GAT TGG GAA AGC GGG TTG AAT GCG ATG GAG GCG GCA CTG CAC CTG GAA AAG AAC GTG AAT CAG TCT CTG CTG GAA CTC CAC AAA TTA GCG ACG GAT AAG AAC GAT CCG CAT CTC GCG GAC TTC ATC GAA ACC CAC TAT TTA AAC GAG CAA GTG AAA GCG ATC AAA GAA CTT GGC GAT CAC GTT ACC AAC CTT CGG AAA ATG GGT GCA CCA GAA AGT GGC TTG GCC GAA TAT CTG TTC GAC AAA CAT ACT CTG GGC GAT TCC GAC AAT GAG TCG Protein sequence: TTASTSQVRQNYHQDSEKAINRQINLELY

			ASYVYLSMSYYFDRDDVALKNFACYFLH QSHEEREHAEKLMKLQNQRGGRIFLQDIQ KPDADDWESGLNAMEAALHLEKNVNQS LLELHKLATDKNDPHLADFIETHYLNEQV KAIKELGDHVTNLRKMGAPESGLAEYLF DKHTLGDSDNES
Ftn^{pos}-A1-1C	21177.59	182	Mutations: K86Q, A18K, C90K, N98R, C102K, H105K, C130A, K53C DNA sequence: ACC ACA GCT AGT ACG TCC CAA GTA CGT CAG AAC TAT CAC CAA GAT AGC GAG AAA GCC ATT AAT CGC CAA ATT AAC TTG GAA CTG TAT GCA TCG TAT GTC TAC CTG TCA ATG AGC TAC TAC TTT GAT CGT GAT GAT GTT GCT CTG AAG AAC TTT GCG TGC TAC TTT CTG CAT CAG TCT CAT GAA GAA CGC GAA CAT GCC GAG AAA CTG ATG AAA CTG CAG AAT CAG CGT GGT GGA CGC ATC TTC TTA CAG GAC ATT CAG AAA CCG GAT AAA GAC GAT TGG GAA AGC GGG TTG CGT GCG ATG GAG AAA GCA CTG AAA CTG GAA AAG AAC GTG AAT CAG TCT CTG CTG GAA CTC CAC AAA TTA GCG ACG GAT AAG AAC GAT CCG CAT CTC GCC GAC TTC ATC GAA ACC CAC TAT TTA AAC GAG CAA GTG AAA GCG ATC AAA GAA CTT GGC GAT CAC GTT ACC AAC CTT CGG AAA ATG GGT GCA CCA GAA AGT GGC TTG GCC GAA TAT CTG TTC GAC AAA CAT

			ACT CTG GGC GAT TCC GAC AAT GAG TCG Protein sequence: TTASTSQVRQNYHQDSEKAINRQINLELY ASYVYLSMSYYFDRDDVALKNFACYFLH QSHEEREHAEKLMKLQNQRGGRIFLQDIQ KPDKDDWESGLRAMEKALKLEKNVNQS LLELHKLATDKNDPHLADFIETHYLNEQV KAIKELGDHVTNLRKMGAPESGLAEYLF DKHTLGDSDNES

Table S2: Protein Identity Confirmation by ESI-MS and MALDI-TOF. The expected mass of ferritin variants was calculated based on the amino acid composition using the Expasy ProtParam tool.[15] The calculated masses $M_{W(Theo)}$ with Rho6G (which has the molar mass $M_{W(Rho6G)}$) are compared to experimentally determined masses $M_{W(Exp)}$ and confirm protein identity and successful coupling of Rho6G for all variants. ΔM is the calculated mass difference between $M_{W(Exp)}$ and $M_{W(Theo)}$ plus $M_{W(Rho6G)}$ ($\Delta M = M_{W(Exp)} - (M_{W(Theo)} + M_{W(Rho6G)})$).

Protein	**$M_{W(Theo)}$ [Da]**	**$M_{W(Rho6G)}$ [Da]**	**$M_{W(Exp)}$ [a] [Da]**	**ΔM [Da]**
Ftn^{neg}-1C	21139.27	636	21775.20	-0.07
HF-1C	20973.23	636	21608.98	-0.26
Ftn^{neg}-m8-1C	21030.28	636	21667.25	+0.97

[a] from ESI-MS measurements

Protein	**$M_{W(Theo)}$ [Da]**	**$M_{W(Rho6G)}$ [Da]**	**$M_{W(Exp)}$ [b] [Da]**	**ΔM [Da]**
Ftn^{pos}-1C	21273.90	636	21911.15	+1.25
Ftn^{pos}-m4-1C	21169.62	636	21807.55	+1.93
Ftn^{pos}-A1-1C	21177.59	636	21813.81	+0.22

[b] from MALDI-MS measurements

For the variant Ftn^{pos}-m4-1C after iron removal disulfide bridges between TGA and some cysteine residues of the protein container were observed in MALDI ($M_{W(Theo)}$ + 90 Da).

References

[1] M. Budiarta, S. Roy, T. Katenkamp, N. Feliu, T. Beck, *Small* **2023**, *19*, 2205606.
[2] L. Lang, H. Böhler, H. Wagler, T. Beck, *Biomacromolecules* **2023**, *25*, 177-187.
[3] M. Künzle, T. Eckert, T. Beck, *J. Am. Chem. Soc.* **2016**, *138*, 12731-12734.
[4] I. Moglia, M. Santiago, Á. Olivera-Nappa, M. Soler, *J. Inorg. Biochem.* **2018**, *183*, 184-190.
[5] E. Jurrus, D. Engel, K. Star, K. Monson, J. Brandi, L. E. Felberg, D. H. Brookes, L. Wilson, J. Chen, K. Liles, et al., *Protein Sci* **2018**, *27*, 112-128.
[6] S. R. Martin, M. J. Schilstra, *Methods Cell Biol* **2008**, *84*, 263-293.
[7] H. Yan, M. Cacioppo, S. Megahed, F. Arcudi, L. Đorđević, D. Zhu, F. Schulz, M. Prato, W. J. Parak, N. Feliu, *Nat. Commun.* **2021**, *12*, 7208.
[8] A. A. de Thomaz, D. B. Almeida, C. L. Cesar, *Quantum Dots: Applications in Biology. Methods in Molecular Biology* **2020**, 85-93.
[9] C. Zeiss, *Applications Manual LSM 510–ConfoCor 2* **2001**.
[10] S. Reindl, A. Penzkofer, *Chem. Phys.* **1996**, *211*, 431-439.
[11] J. H. Smit, J. H. van der Velde, J. Huang, V. Trauschke, S. S. Henrikus, S. Chen, N. Eleftheriadis, E. M. Warszawik, A. Herrmann, T. Cordes, *PCCP* **2019**, *21*, 3721-3733.
[12] A. D. Gonçalves, C. Alexander, C. J. Roberts, S. G. Spain, S. Uddin, S. Allen, *RSC Adv.* **2016**, *6*, 15143-15154.
[13] F. Otto, F. Dallari, F. Westermeier, D. F. Wieland, W. J. Parak, F. Lehmkühler, F. Schulz, *Aggregate* **2024**, e483.
[14] O. Vilanova, J. J. Mittag, P. M. Kelly, S. Milani, K. A. Dawson, J. O. Rädler, G. Franzese, *ACS nano* **2016**, *10*, 10842-10850.
[15] E. Gasteiger, A. Gattiker, C. Hoogland, I. Ivanyi, R. D. Appel, A. Bairoch, *Nucleic Acids Res.* **2003**, *31*, 3784-3788.